ARTICLES

Journal of Semiconductors
(2023) 44, 112301
doi: 10.1088/1674-4926/44/11/112301

Modulation bandwidth enhancement in monolithic integrated two-section DFB lasers based on the detuned loading effect

Yunshan Zhang[1], Yifan Xu[1], Shijian Guan[2], Jilin Zheng[3], Hongming Gu[1], Lianyan Li[1], Rulei Xiao[2], Tao Fang[2], Hui Zou[1], and Xiangfei Chen[2, †]

[1]College of Electronic and Optical Engineering and College of Flexible Electronics (Future Technology), Nanjing University of Posts and Telecommunications, Nanjing 210023, China

[2]College of Engineering and Applied Sciences, Nanjing University, Nanjing 210023, China

[3]College of Communications Engineering, PLA Army Engineering University, Nanjing 210007, China

Abstract: Modulation bandwidth enhancement in a directly modulated two-section distributed feedback (TS-DFB) laser based on a detuned loading effect is investigated and experimentally demonstrated. The results show that the 3-dB bandwidth of the TS-DFB laser is increased to 17.6 GHz and that chirp parameter can be reduced to 2.24. Compared to the absence of a detuned loading effect, there is a 4.6 GHz increase and a 2.45 reduction, respectively. After transmitting a 10 Gb/s non-return-to-zero (NRZ) signal through a 5-km fiber, the modulation eye diagram still achieves a large opening. Eight-channel laser arrays with precise wavelength spacing are fabricated. Each TS-DFB laser in the array has side mode suppression ratios (SMSR) > 49.093 dB and the maximum wavelength residual < 0.316 nm.

Key words: distributed feedback (DFB) laser; detuned loading effect; direct modulation

Citation: Y S Zhang, Y F Xu, S J Guan, J L Zheng, H M Gu, L Y Li, R L Xiao, T Fang, H Zou, and X F Chen, Modulation bandwidth enhancement in monolithic integrated two-section DFB lasers based on the detuned loading effect[J]. *J. Semicond.*, 2023, 44(11), 112301. https://doi.org/10.1088/1674-4926/44/11/112301

1. Introduction

The continuous increase in data traffic increases the pressure on data centers to transmit information. Directly modulated lasers (DMLs) have attracted great interest in optical communication systems for high-efficiency, low-power consumption, small size, and cost effectiveness, which makes it valuable to enhance their modulation bandwidth.

High-speed DMLs require a large relaxation oscillation frequency, and this parameter is related to the differential gain and the volume of the active region. High-speed DMLs widely adopt AlGaInAs multi-quantum well (MQW) active regions to increase differential gain[1–8]. In addition, the relaxation oscillation frequency can also be enhanced by reducing the volume of the active region, such as using a buried heterostructure (BH)[3, 4] and reducing the laser cavity length[5–8]. Since less feedback in the short cavity will lead to higher threshold gain, high-reflection (HR) coating is inevitable to increase optical feedback. However, the grating at the HR-coated facet has an uncontrollable random phase shift, which has a great impact on the single longitudinal mode (SLM) yield and the wavelength accuracy[9], and it is not conducive to the manufacture of DFB laser arrays. Anti-reflection (AR) coatings can be used to eliminate the influence of random phase, but the modulation bandwidth and output efficiency will deteriorate. Besides, the direct modulation bandwidth can also be extended by a detuned loading effect[10–12] and a photon–photon resonance effect[13–15]. But the integration between the active and passive regions makes chip manufacturing difficult and costly. In this paper, we propose a directly modulated two-section DFB (TS-DFB) laser with an enhanced modulation bandwidth using the detuned loading effect. The reconstruction equivalent chirp (REC) technique is used to fabricate the TS-DFB lasers and TS-DFB laser arrays. The REC technique can implement various complicated grating structures equivalently with simple manufacturing processes and low costs[16–18]. In this device there are two sections, one is used as a normal DFB laser and the other as a grating reflector. Both gratings in both sections are sampled Bragg gratings (SBGs) manufactured with the REC technique. Through tuning sampling periods of SBGs, the frequency detuning between the SBGs of two sections is achieved, then the detuned loading effect is obtained. Utilizing the detuned loading effect, the 3-dB bandwidth of the TS-DFB laser is enhanced from 13 GHz to 17.6 GHz and the chirp parameter of 4.69 is reduced to 2.24. A clear eye pattern is observed when a 10 Gb/s non-return-to-zero (NRZ) signal is applied. Furthermore, the eye pattern can still maintain a large opening extent after 5 km single-mode fiber transmission.

2. Principle, design, and fabrication

Fig. 1 shows the schematic of the proposed TS-DFB lasers. The conventional two-stage metal–organic chemical vapor deposition (MOCVD) is employed for its fabrication. An electrical isolation is achieved by removing a 20 μm long ohmic contact layer between two sections. Therefore, different currents I_1 and I_2 can be independently injected into Section Ⅰ and Section Ⅱ. Two sections are used as a common DFB laser and a grating reflector with lengths of 400 and

Correspondence to: X F Chen, chenxf@nju.edu.cn
Received 13 MAY 2023; Revised 14 JUNE 2023.

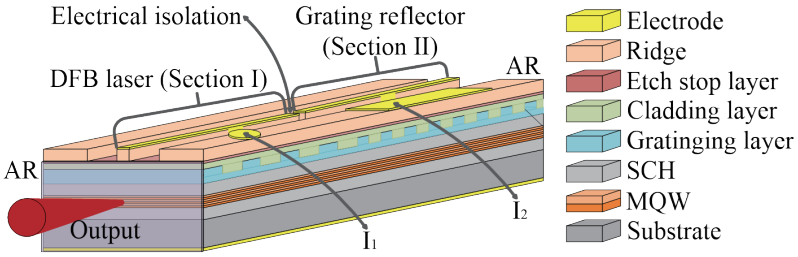

Fig. 1. (Color online) Schematic of the proposed TS-DFB laser.

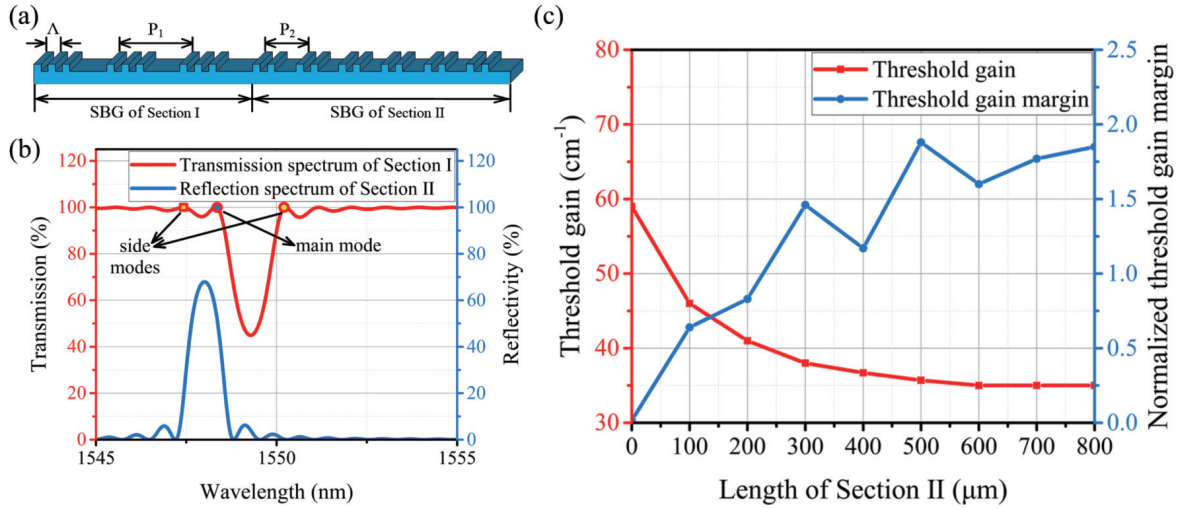

Fig. 2. (Color online) (a) Schematic of the SBGs in TS-DFB lasers. (b) Reflection and transmission spectra of SBGs in different sections. (c) Threshold gain and threshold gain margin versus the length of the grating reflector.

500 μm, respectively. In the first epitaxial growth, the lower separate-confinement-heterostructure (SCH) layer, MQW active region and the upper SCH layer are grown on the n-InP substrate. The SBG is then fabricated by the holographic exposure combined with conventional photolithography, with an effective coupling coefficient of 35 cm^{-1}. After the fabrication of the SBGs, the cladding layer and stop layer are regrown on the chip. Then the ridge waveguide processing is executed. Section Ⅰ adopts a small-area electrode to reduce the influence of parasitic capacitance on the modulation characteristics. Lastly, both facets of the device are deposited with AR coatings with a reflectivity of less than 1%.

When fabricating complex grating structures, relatively high-cost and time-consuming methods such as electron-beam lithography are required[19]. By designing the sampling period of SBGs, the REC technique can fabricate a variety of gratings with complicated structures. The detailed principles of the REC technique can be found in Ref. [20, 21]. The structure schematic of SBGs in the TS-DFB laser is shown in Fig. 2(a). The SBGs in both sections are uniform sampled gratings, which have the same seed grating period Λ and different sampling periods. By changing the sampling periods of SBGs in two sections, labeled as P_1 and P_2 respectively, different Bragg wavelengths of the SBGs in the two sections with high precision are obtained, and it is essential for the detuned loading effect. The transmission and reflection spectra of two sections are shown in Fig. 2(b). There are two eigenmodes on both sides of the stopband of gratings in Section Ⅰ, leading to serious mode competition. In order to achieve the detuned loading effect, one of the two eigenmodes should be located at the falling edge of the gratings reflection spectrum in Section Ⅱ. Besides, the other eigenmode is outside the reflection spectrum. Therefore, the eigenmode of the short wavelength side obtains a higher reflectivity from the grating reflector compared to that of the longer wavelength side. As shown in Fig. 2(c), the threshold gain of the main mode can be reduced by the optical feedback from Section Ⅱ, and it becomes saturated when the length of the grating reflector exceeds 500 μm. In addition, the use of the grating reflector greatly improves the threshold gain margin compared to a conventional AR coated DFB laser, which means the SLM yield is improved.

Moreover, the detuned loading effect can improve the modulation properties. For multi-section lasers, the rate equation of photons can be written as[22]

$$\frac{\mathrm{d}S}{\mathrm{d}t} = \left[\Gamma v_{\mathrm{g}} g - \alpha_{\mathrm{i}} - \alpha_{\mathrm{m}} + \frac{1}{2}\frac{\mathrm{d}\ln(K_z)}{\mathrm{d}t}\right] S, \tag{1}$$

where S is the photon density, v_{g} is the group velocity, Γ is the confinement factor, g is lthe gain, K_z is the longitudinal Petermann factor, and α_{i} and α_{m} are internal loss and mirror loss, respectively. The expression of the resonance frequency can be obtained by the small signal expansion of the rate equation, which can be expressed as

$$f_{\mathrm{t}} = \frac{1}{2\pi}\sqrt{\left(\alpha_{\mathrm{i}} + \alpha_{\mathrm{m}}\right) S \frac{\partial}{\partial N}\left(\Gamma v_{\mathrm{g}} g - \alpha_{\mathrm{i}} - \alpha_{\mathrm{m}}\right)}, \tag{2}$$

where N represents the carrier density. As shown in Fig. 3, the detuning of the SBG between the two sections and the

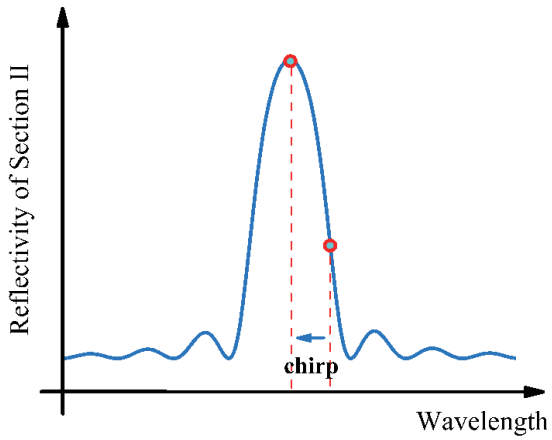

Fig. 3. (Color online) The principle of the detuned loading effect in TS-DFB lasers. Circles represent the main mode.

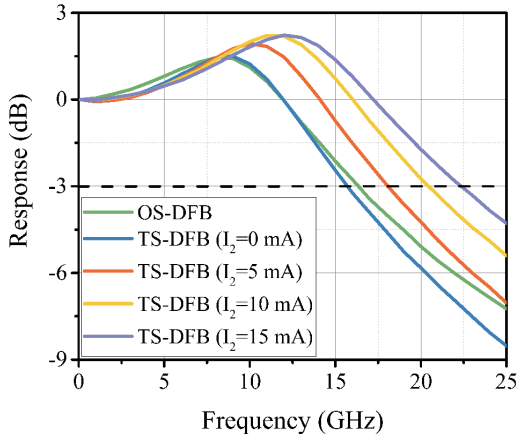

Fig. 4. (Color online) Calculated small-signal modulation response of the TS-DFB laser and OS-DFB laser.

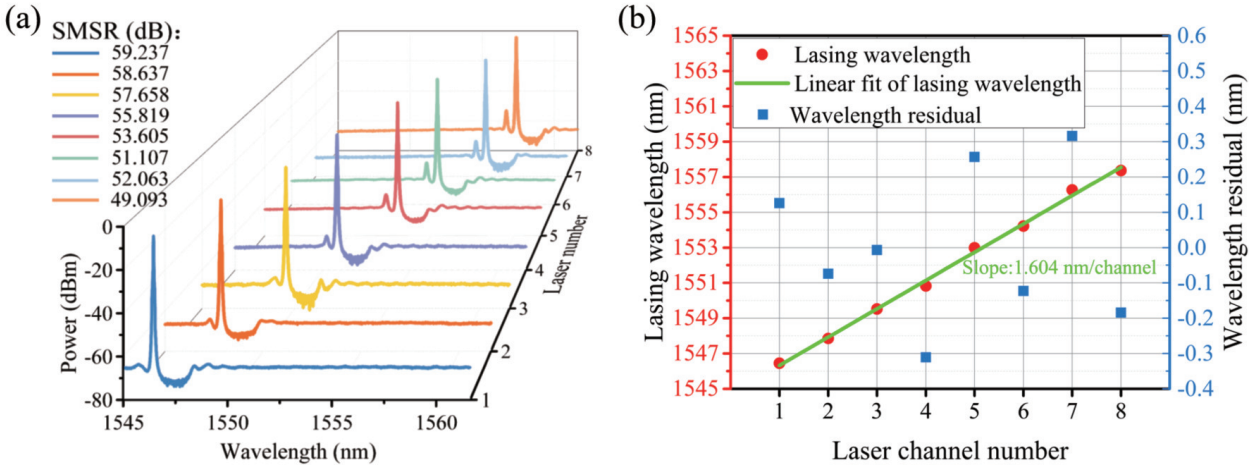

Fig. 5. (Color online) (a) Measured spectra of the eight-channel TS-DFB laser array (I_1 = 70 mA, I_2 = 25 mA). (b) The corresponding lasing wavelengths of laser arrays (dots). The linear fitting line of wavelengths, and the residuals after fitting.

Joule heat caused by the current injection in Section Ⅰ will move the main mode to the falling edge of the reflection spectrum of Section Ⅱ. In this situation, the frequency up-chirp under modulation will shift the main mode closer to the reflection peak of the grating reflector. As a result, the increase of the longitudinal confinement factor and the decrease of the mirror loss cause an increase in the effective differential gain, which can be easily concluded from Eq. (2). Therefore, the relaxation oscillation frequency can be enhanced by the detuned loading effect[23].

Fig. 4 shows the simulated response curves when I_1 is 100 mA. The small-signal modulation response of a one-section DFB (OS-DFB) laser with the length of 400 μm is also shown for comparison. When the bias current of Section Ⅱ is tuned from 0 to 15 mA, the modulation bandwidth of the TS-DFB laser increases from 15.5 to 22 GHz. Through injecting current into Section Ⅱ, not only the loss of grating reflector can be gradually compensated, but its reflectivity is also enhanced. In addition, due to the decrease in the effective index of Section Ⅱ with the increase in the I_2, the main mode will be moved to the steeper falling edge of the grating reflector and so the detuned loading effect can be enhanced. As a result, the relaxation oscillation frequency is increased. The 3-dB bandwidth is improved to 22 GHz, while that of the OS-DFB laser is only 16 GHz.

3. Experimental results

3.1. Characteristics of the eight-channel TS-DFB laser array

An eight-channel TS-DFB laser array chip is fabricated using the proposed method, with a wavelength spacing of 1.6 nm. Fig. 5(a) shows the lasing spectra of eight TS-DFB lasers in the array under the same bias current I_1 = 70 mA and I_2 = 25 mA. To compensate the loss in the grating reflector, I_2 is set under the threshold current to avoid laser lasing. The laser arrays have excellent SLM yield and the smallest SMSR of the eight lasers is larger than 49 dB. As shown in Fig. 5(b), the average wavelength separation of channels is 1.604 nm, with an average error of only 0.004 nm compared to the designed spacing value of 1.6 nm. The maximum wavelength residual is 0.316 nm.

Fig. 6(a) shows the measured output power of the eight-channel array with the same injection condition I_2 = 25 mA. The threshold currents of eight lasers ranges from 26.5 to 29.2 mA, and the slope efficiency varies between 0.125 and 0.157 W/A. Fig. 6(b) shows the influence of injection current I_2 on light-current characteristics. Obviously, when there is no current injection in Section Ⅱ, the mode competition is serious, and mode hopping occurs during the process of adjusting the current. It is obvious that the reflector section can not

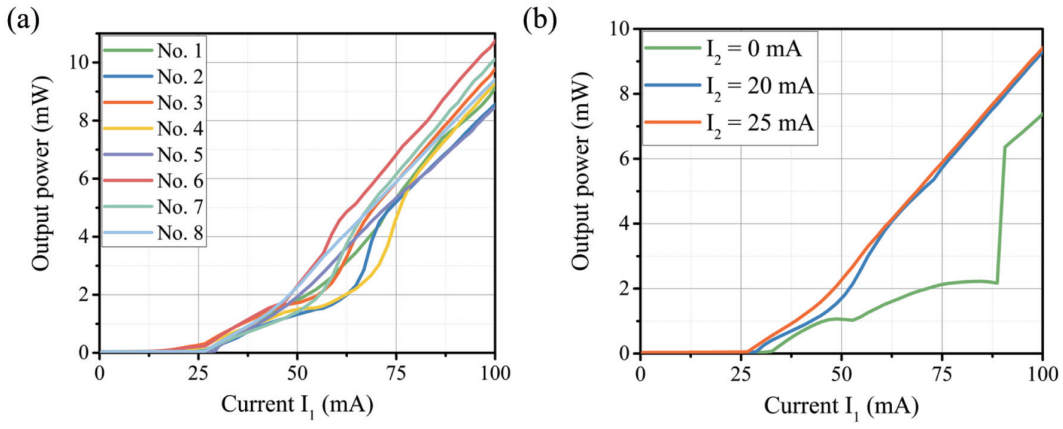

Fig. 6. (Color online) Light-current characteristics of (a) the TS-DFB laser array and (b) the TS-DFB laser with different current I_2.

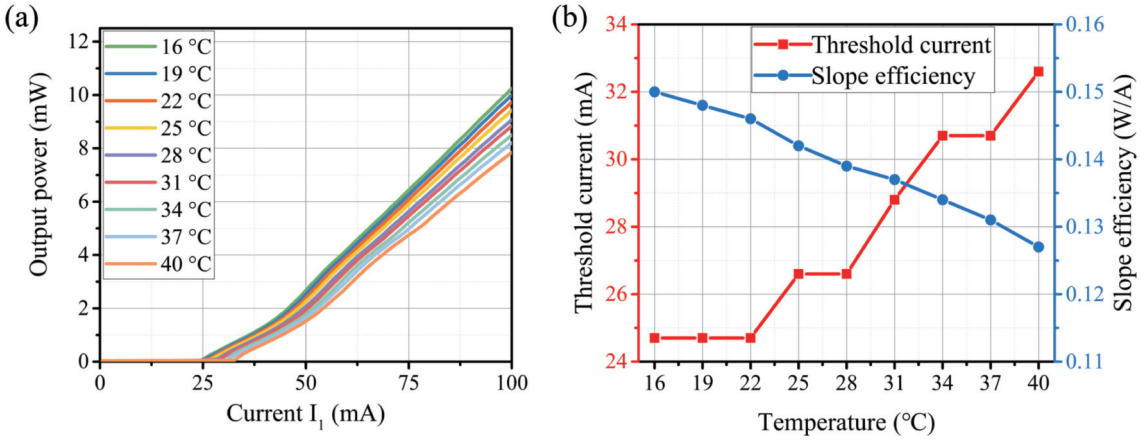

Fig. 7. (Color online) (a) Light-current characteristics with different temperatures when I_2 is 25 mA. (b) Corresponding threshold current and slope efficiency.

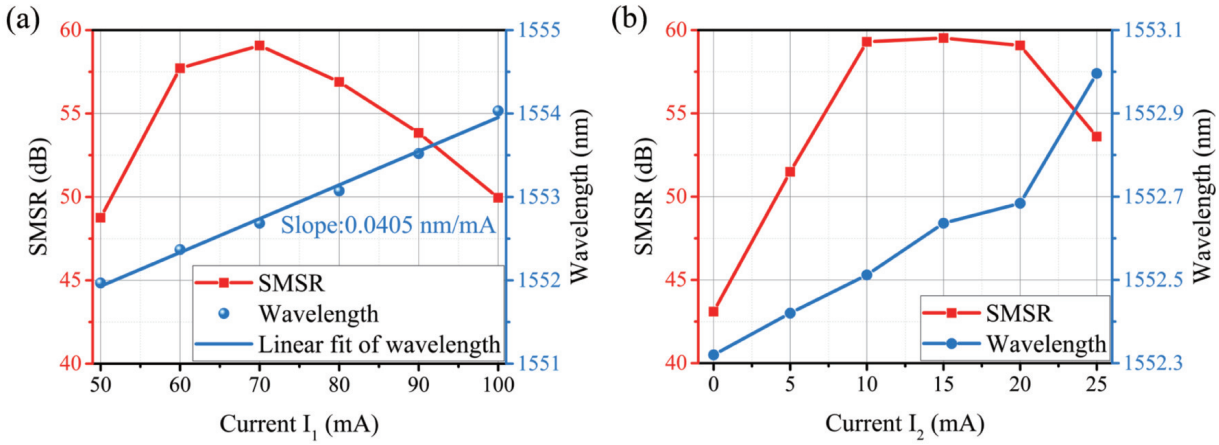

Fig. 8. (Color online) Measured SMSRs and lasing wavelengths. (a) I_1 = 50–100 mA, I_2 = 20 mA and (b) I_2 = 0–25 mA, I_1 = 70 mA.

only improve the SLM performance, but also can increase the slope efficiency and reduce the threshold current of the TS-DFB lasers. As I_2 increases from 0 to 25 mA, the threshold current is reduced from 32.6 to 26.6 mA.

The above measurements are carried out at room temperature (25 °C). To investigate the influence of temperature on light-current characteristics, the temperature is tuned from 16 to 40 °C and the data is recorded at 3 °C intervals. As illustrated in Fig. 7(a), the power and current maintain a good linear relationship under different temperature conditions. The threshold current and slope efficiency are 26.6 mA and 0.142 W/A at room temperature, respectively. As shown in Fig. 7(b), the threshold current increases from 24.7 to 32.6 mA and the slope efficiency decreases from 0.15 to 0.127 W/A when the temperature varies from 16 to 40 °C.

One of the channels is chosen to study the influence of injection current I_1 and I_2 on the SMSR and lasing wavelength, as illustrated in Fig. 8(a). The TS-DFB laser maintains good SLM operation when I_1 is tuned from 50 to 100 mA, and SMSR remains consistently above 48 dB. The injection of I_1 redshifts the Bragg wavelength, so that the short wavelength eigenmode gains a larger reflection compared to the long wavelength eigenmode, and therefore the SMSR increases. As I_1 increases further, the side mode of Section I

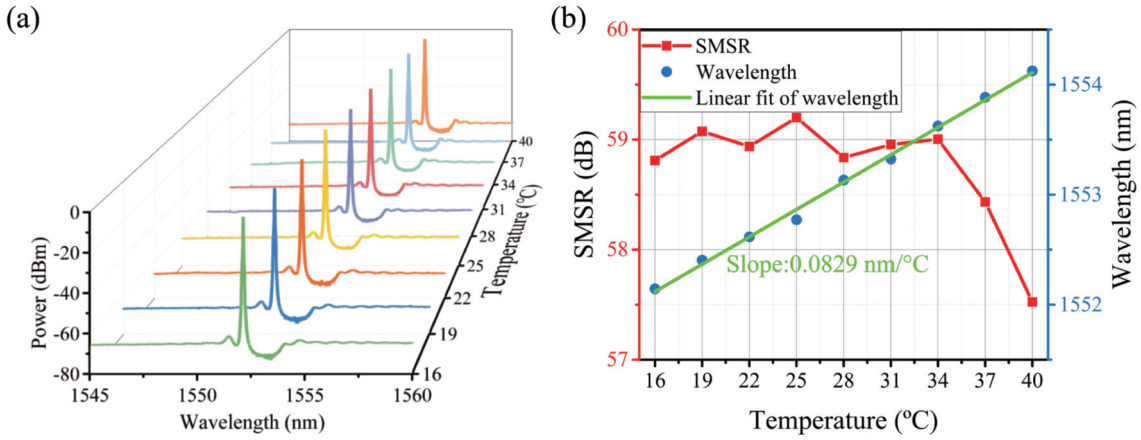

Fig. 9. (Color online) (a) Measured spectra at different temperatures when I_1 is 70 mA and I_2 is 20 mA. (b) The corresponding SMSRs and lasing wavelengths.

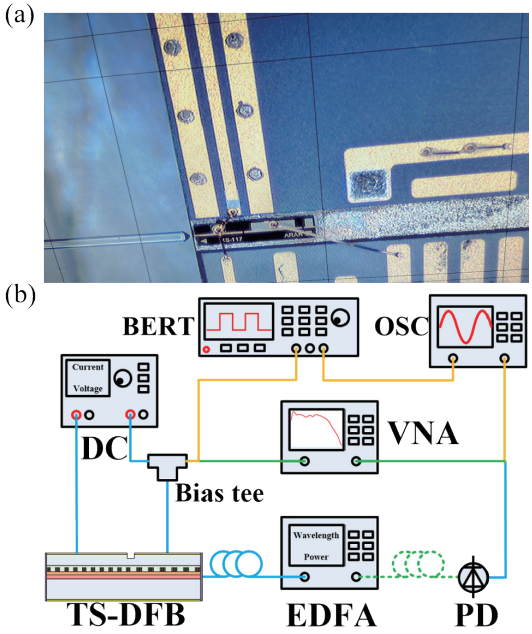

Fig. 10. (Color online) (a) Photo of the TS-DFB laser on the carrier. (b) Experimental setup schematic for the measurement of dynamic characteristics. EDFA: erbium-doped fiber amplifier, OSC: oscilloscope, DC: direct-current power source, BERT: bit error rate tester, VNA: vector network analyzer, PD: photodetector.

also gains a large reflectivity, so the SMSR is reduced. Besides, the increase of I_1 results in Joule heating in the Section Ⅰ, which causes the red shift of the lasing wavelength. The lasing wavelength is varied from 1551.968 to 1554.032 nm with a range of 2.064 nm. The rate of change is around 0.0405 nm/mA. As illustrated in Fig. 8(b), the increase of I_2 can increase the SMSR and suppress mode competition, due to the reflectivity enhancement of the SBG in Section Ⅱ, which provides higher reflection for the short wavelength eigenmode. The SMSRs are higher than 50 dB when I_2 is larger than 5 mA. As I_2 approaches the threshold current, the mode of Section Ⅱ becomes visible and the SMSR decreases. In addition, the varying of I_2 can change the refractive index of the device, resulting in the tuning of the lasing wavelength. The wavelength is increased from 1552.32 to 1552.996 nm when I_2 is varied from 0 to 25 mA, with a tuning range of 0.676 nm.

To investigate the influence of temperature on lasing characteristics, spectra are measured at different temperatures when I_1 is 70 mA and I_2 is 20 mA. Fig. 9(a) shows that the stable SLM operation of the TS-DFB laser is obtained under different temperature conditions. Extremely high SMSRs are achieved, all above 57.5 dB. Similarly, as the temperature increases, the lasing wavelength moves to longer wavelengths, changing from 1552.144 to 1554.124 nm with a range of 1.98 nm. The rate of change is about 0.0829 nm/°C.

3.2. Dynamic characteristics of the TS-DFB laser

A TS-DFB laser is mounted on the carrier to investigate its dynamic characteristics, as illustrated in Fig. 10(a). Fig. 10(b) gives the experimental setup for the dynamic characteristic measurement. The high-frequency signal of the vector network analyzer (VNA), or bit error rate tester (BERT) and the current of the DC power source are fed into TS-DFB laser by the carrier. The BERT is used to provide a digital signal to the laser so that the eye diagram can be observed from the oscilloscope (OSC).

The response curves of the TS-DFB laser under different injection conditions are given in Fig. 11. The direct modulation bandwidth increases from 14.7 to 17.6 GHz when I_1 is changed from 60 to 100 mA and I_2 is set to 25 mA constantly. Fig. 11(b) shows the effect of I_2 on the 3-dB bandwidth. When Section Ⅱ is unbiased, the modulation bandwidth is only about 13 GHz. However, when Section Ⅱ is biased with a current of 25 mA, the detuned loading effect increases the 3-dB bandwidth to 17.6 GHz.

Furthermore, the chirp parameter is also a significant quantity of the optical transmission systems. The applications of DML at 1.55 μm wavelength are limited partially owing to the large dispersion of the fiber. The poor dispersion tolerance is caused by the large chirp parameter of DML. In order to measure the chirp parameter, the method in Ref. [24] is used. Fig. 12 shows the measured and calculated chirp parameter under different injection conditions. When I_1 = 100 mA and I_2 is tuned from 0 to 25 mA, the chirp parameter is reduced from 4.69 to 2.24 due to detuned loading effect. Besides, from another line it can be seen that the increase of I_1 also reduces the chirp parameter, from 3.17 to 2.24. This is because the Joule heating shifts the main mode to the steeper falling edge of grating reflector, enhancing the detuned loading effect.

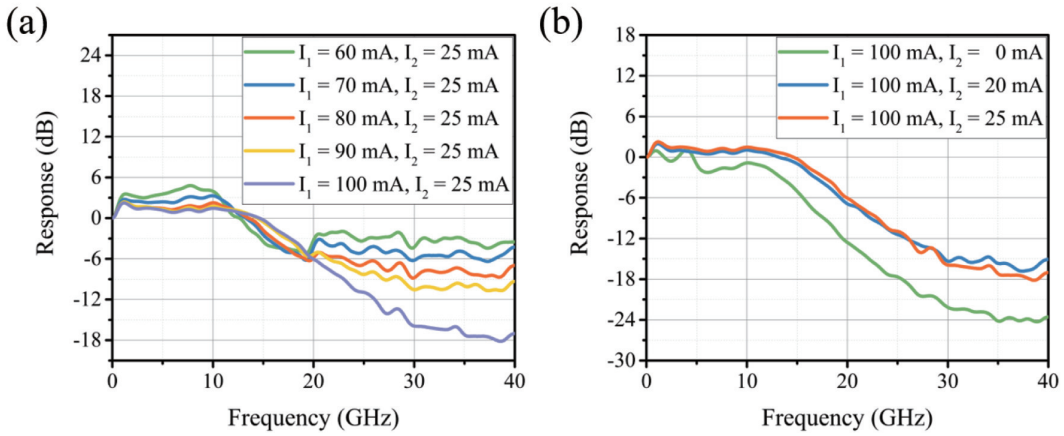

Fig. 11. (Color online) Small-signal modulation response of the TS-DFB laser. (a) I_1 = 60–100 mA, I_2 = 25 mA. (b) I_2 = 0–25 mA, I_1 = 100 mA.

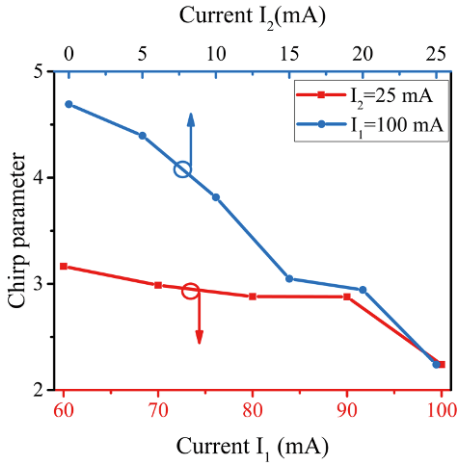

Fig. 12. (Color online) Measured chirp parameters at different currents.

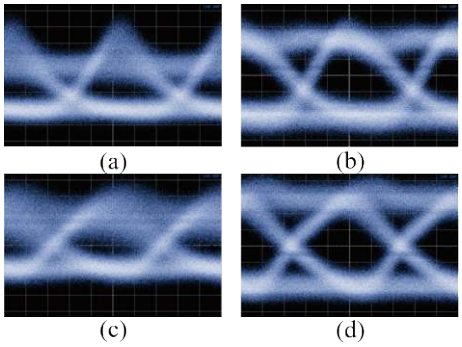

Fig. 13. (Color online) Eye diagrams under 10 Gb/s direct modulation after back-to-back (BTB) and 5 km single mode fiber transmission. (a) BTB, I_2 = 0 mA. (b) BTB, I_2 = 25 mA. (c) 5 km, I_2 = 0 mA. (d) 5 km, I_2 = 25 mA.

A 10 Gb/s NRZ signal is used to modulate the TS-DFB laser directly. For comparison, I_1 is fixed at 100 mA, and I_2 is 0 and 25 mA, respectively. Figs. 13(a) and 13(b) are the eye diagrams of back-to-back (BTB) transmission under direct modulation. When there is no current injection in Section Ⅱ, the eye diagram is not ideal. By contrast, clear eye-openings and large opening extent are obtained when I_2 is 25 mA. This is due to the enhanced modulation bandwidth caused by the detuned loading effect. The extinction ratios of the two eye diagrams are 2.96 and 4.09 dB, respectively. To verify the reduction of chirp parameter, the eye diagrams after 5 km

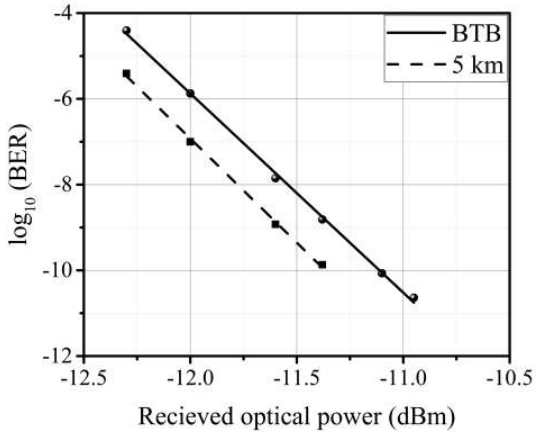

Fig. 14. The measured BER under 10 Gb/s NRZ modulation when I_2 is 25 mA.

fiber transmission are recorded, as shown in Figs. 13(c) and 13(d). Compared with Fig. 13(a), the opening extent of the eye diagram is deteriorated due to the large chirp parameter when Section Ⅱ is unbiased. However, when I_2 is 25 mA, only slight dispersion is observed, and a clear eye-opening can still be obtained. The extinction ratios of the two eye diagrams are 2.62 and 3.72 dB, respectively. Therefore, the chirp is effectively suppressed due to detuned loading effect, which is helpful for signal transmission.

Fig. 14 shows the measured bit error rate (BER) for 10 Gb/s NRZ operation. The current I_2 is set at 25 mA to achieve detuned loading effect. The BER characteristics for BTB configuration and 5 km single mode fiber transmission at different optical powers are given. By increasing the optical power, the BER can be reduced to less than 10^{-9}. In addition, the eye diagram is optimized by fiber dispersion, resulting in a lower BER after 5 km transmission for the same optical power.

4. Conclusion

A direct modulation two-section DFB laser based on the REC technique is proposed and investigated. Using this structure, an eight-channel laser array is manufactured. The array has stable SLM operation and precise wavelength spacing. The average wavelength error of the channels is only 0.004 nm. High SMSR over 49 dB is achieved. The threshold current and slope efficiency can also be improved through changing the bias current on the grating reflector section. At different temperature conditions, the TS-DFB laser owns

good stability. In addition, dynamic characteristics, including the small-signal modulation response and chirp of the TS-DFB laser, are also analyzed experimentally. The 3-dB modulation bandwidth of 13 GHz increases to 17.6 GHz and the chirp parameter of 4.69 is reduced to 2.24 due to the detuned loading effect. Direct modulation is performed with a 10 Gb/s NRZ signal and clear eye-openings are observed. Owing to chirp suppression, a clear eye-opening can still be obtained after 5 km of single-mode fiber transmission.

Moreover, by optimizing the coupling coefficient of grating, laser cavity length, waveguide structure or epitaxial material, further improvements can be achieved. For instance, reducing the laser length or using the BH. The adoption of this structure and the REC technique greatly reduces the fabrication cost of laser chips, and the good static and dynamic characteristics make it a promising light source for optical communication systems.

References

[1] Ishikawa T, Higashi T, Uchida T, et al. Evaluation of differential gain of 1.3/spl mu/m AlGaInAs/InP strained MQW lasers. Conference Proceedings. 1998 International Conference on Indium Phosphide and Related Materials (Cat. No. 98CH36129), 2002, 729

[2] Morthier G. Design and optimization of strained-layer-multi-quantum-well lasers for high-speed analog communications. IEEE J Quantum Electron, 1994, 30, 1520

[3] Otsubo K, Matsuda M, Takada K, et al. 1.3-μm AlGaInAs multiple-quantum-well semi-insulating buried-heterostructure distributed-feedback lasers for high-speed direct modulation. IEEE J Sel Top Quantum Electron, 2009, 15, 687

[4] Nakahara K, Wakayama Y, Kitatani T, et al. Direct modulation at 56 and 50 Gb/s of 1.3-μm InGaAlAs ridge-shaped-BH DFB lasers. IEEE Photonics Technol Lett, 2015, 27, 534

[5] Kobayashi W, Tadokoro T, Ito T, et al. High-speed operation at 50 Gb/s and 60-km SMF transmission with 1.3-μm InGaAlAs-based DML. ISLC 2012 International Semiconductor Laser Conference, 2012, 50

[6] Sakaino G, Takiguchi T, Sakuma H, et al. 25.8Gbps direct modulation of BH AlGaInAs DFB lasers with p-InP substrate for low driving current. 22nd IEEE International Semiconductor Laser Conference, 2010, 197

[7] Tadokoro T, Kobayashi W, Fujisawa T, et al. 43 Gb/s 1.3 μm DFB laser for 40 km transmission. J Light Technol, 2012, 30, 2520

[8] Uetake A, Otsubo K, Matsuda M, et al. 40-Gbps direct modulation of 1.55-μm AlGaInAs semi-insulating buried-heterostructure distributed reflector lasers up to 85°C. 2009 IEEE LEOS Annual Meeting Conference Proceedings, 2009, 839

[9] Henry C. Performance of distributed feedback lasers designed to favor the energy gap mode. IEEE J Quantum Electron, 1985, 21, 1913

[10] Matsui Y, Schatz R, Che D. Isolator-free > 67-GHz bandwidth DFB+R laser with suppressed chirp. 2020 Optical Fiber Communications Conference and Exhibition, 2020, 1

[11] Che D, Matsui Y, Schatz R, et al. Direct modulation of a 54-GHz distributed Bragg reflector laser with 100-GBaud PAM-4 and 80-GBaud PAM-8. 2020 Optical Fiber Communications Conference and Exhibition (OFC), 2020, 1

[12] Guan S J, Zhang Y S, Zheng J L, et al. Modulation bandwidth enhancement and frequency chirp suppression in two-section DFB laser. J Light Technol, 2022, 40, 7383

[13] Zhao W, Mao Y F, Lu D, et al. Modulation bandwidth enhancement of monolithically integrated mutually coupled distributed feedback laser. Appl Sci, 2020, 10, 4375

[14] Yamaoka S, Diamantopoulos N P, Nishi H, et al. Directly modulated membrane lasers with 108 GHz bandwidth on a high-thermal-conductivity silicon carbide substrate. Nat Photonics, 2021, 15, 28

[15] Matsui Y, Schatz R, Che D, et al. Low-chirp isolator-free 65-GHz-bandwidth directly modulated lasers. Nat Photonics, 2021, 15, 59

[16] Yuan B C, Shi J Q, Qi W X, et al. A monolithic integrated dual-wavelength DFB laser with equivalent inverse-Gaussian apodized grating. IEEE Photonics J, 2020, 12, 1

[17] Guan S J, Zhang Y S, Yuan B C, et al. Research on the asymmetric corrugation-pitch-modulated HR-AR DFB lasers with sampled gratings. J Light Technol, 2021, 39, 4725

[18] Zhang Y S, Yuan B C, Shi J Q, et al. A stable dual-wavelength DFB semiconductor laser with equivalent chirped sampled grating. IEEE J Quantum Electron, 2022, 58, 1

[19] Vieu C, Carcenac F, Pépin A, et al. Electron beam lithography: Resolution limits and applications. Appl Surf Sci, 2000, 164, 111

[20] Dai Y T, Chen X F, Xia L, et al. Sampled Bragg grating with desired response in one channel by use of a reconstruction algorithm and equivalent chirp. Opt Lett, 2004, 29, 1333

[21] Sun Z X, Xiao R L, Zhao Y, et al. Design of four-channel wavelength-selectable In-series DFB laser array with 100-GHz spacing. J Light Technol, 2020, 38, 2299

[22] Bandelow U, Schatz R, Wunsche H J. A correct single-mode photon rate equation for multisection lasers. IEEE Photonics Technol Lett, 1996, 8, 614

[23] Chaciński M, Schatz R. Impact of losses in the Bragg section on the dynamics of detuned loaded DBR lasers. IEEE J Quantum Electron, 2010, 46, 1360

[24] Devaux F, Sorel Y, Kerdiles J F. Simple measurement of fiber dispersion and of chirp parameter of intensity modulated light emitter. J Light Technol, 1993, 11, 1937

Yunshan Zhang received the B.S. degree in science and technology of electronics from Shandong University in 2002, and the Ph.D. degree in physical electronics from the Beijing Institute of Technology in 2011. From 2013 to 2015, he was a Post-Doctoral Researcher with the College of Engineering and Applied Sciences, Nanjing University. He is currently an Associate Professor with the Nanjing University of Posts and Telecommunications. His research interests include solid state lasers, DFB semiconductor lasers, fiber communication, and photonic integrated circuits.

Xiangfei Chen received the B.S. degree in physics from Soochow University in 1991, and the M.S. and Ph.D. degrees in physics from the Nanjing University in1993 and 1996, respectively. From 1996 to 2000, he was a Faculty Member with the Nanjing University of Posts and Telecommunications. From 2000 to 2006, he served as an Associate Professor with the Department of Electrical Engineering, Tsinghua University. From October 2004 to April 2005, he was a Visiting Scholar with the Microwave Photonics Research Laboratory, School of Information Technology and Engineering, University of Ottawa. He is currently a Professor with the Microwave Photonics Technology Laboratory, National Laboratory of Microstructures, and the College of Engineering and Applied Sciences, Nanjing University. His research interests include development of novel optical devices for high-speed large-capacity optical networks, microwave photonic systems, and fiber-optic sensors.